CHEMISTRY OF MATERIALS

pubs.acs.org/cm

Article

Exploring the Links between Structural Distortions, Orbital Ordering, and Multipolar Magnetic Ordering in Double Perovskites Containing Re(VI) and Os(VII)

Published as part of Chemistry of Materials special issue "In Memory of Prof. Francis DiSalvo".

Victor da Cruz Pinha Barbosa, Dalini D. Maharaj, Zachery W. Cronkright, Ye Wang, Rong Cong, Erick Garcia, Arneil P. Reyes, Jiaqiang Yan, Clemens Ritter, Vesna F. Mitrović, Bruce D. Gaulin, John E. Greedan, and Patrick M. Woodward*

Cite This: *Chem. Mater.* 2024, 36, 11478−11489

Read Online

ACCESS | Metrics & More | Article Recommendations | Supporting Information

ABSTRACT: A combination of high-resolution powder diffraction techniques and solid-state NMR has been employed to explore the links between crystal structure, orbital ordering, and magnetism in three isostructural double perovskites containing transition metal ions with a $5d^1$ configuration. In Ba_2ZnReO_6, both neutron and synchrotron X-ray powder diffraction data reveal a cubic-to-tetragonal transition at 23 K that breaks the degeneracy of the t_{2g} orbitals and leads to a pattern of orbital ordering that stabilizes magnetic ordering when the sample is cooled below 16 K. Similar behavior is observed in Ba_2MgReO_6, with an orbital ordering temperature of 33 K and a magnetic ordering temperature of 18 K. Prior theoretical works suggest that the pattern of orbital order seen in the $P4_2/mnm$ space group is needed to stabilize the heavily canted antiferromagnetism of these compounds. Unfortunately, powder diffraction data is not sensitive enough to differentiate between the $I4/mmm$ and $P4_2/mnm$ structural models, as the distortions are too subtle to be unambiguously identified from either neutron or synchrotron X-ray powder diffraction methods. In contrast, both diffraction and ^{7}Li NMR data indicate that Ba_2LiOsO_6 retains the cubic structure down to 1.7 K. The antiferromagnetic ground state and lack of any sign of orbital ordering in Ba_2LiOsO_6 provide compelling evidence that the electronically driven tetragonal distortion seen in Ba_2ZnReO_6, and Ba_2MgReO_6 is intimately linked to the magnetic ordering seen in those compounds. The absence of magnetic reflections in high intensity neutron powder diffraction data collected on Ba_2MgReO_6 strongly suggests ordering of multipolar moments on Re(VI), likely ferro-octupolar ordering.

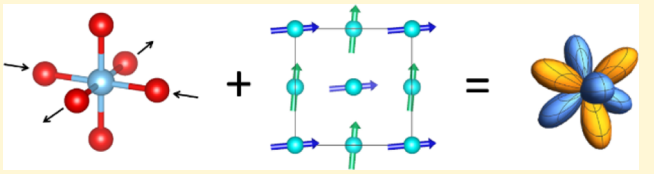

INTRODUCTION

Double perovskites containing $5d^1$ ions are characterized by competing magnetic ground states. Examples have been reported that exhibit collinear antiferromagnetic ordering (e.g., Ba_2LiOsO_6), heavily canted antiferromagnetic ordering with a substantial net magnetization (e.g., Ba_2NaOsO_6), and spin freezing into a glassy magnetic state (e.g., Sr_2LiOsO_6).[1−5] Subtle changes in spin−orbit coupling, superexchange interactions, intersite Coulomb repulsion, and/or structural distortions all seem to impact this competition. Even more exotic states involving strong spin−orbit entanglement leading to multipolar (quadrupolar, octupolar) local magnetic moments have also been proposed.[6,7]

Theoretical studies predict that preferential occupation of specific d-orbitals, what a chemist would call orbital ordering, is an important driver of the low temperature magnetism of these materials.[6,7] Note that the term *orbital ordering*, which is appropriate for treating spin−orbit coupling in the LS basis, is equivalent to the term *quadrupolar ordering*, when spin−orbit coupling is treated in the J basis. Both terms can be found in the literature, but here we predominantly use orbital ordering as it more clearly conveys the forces that drive this phase transition. The onset of orbital order is thought to stabilize an unusual heavily canted antiferromagnetic state in double perovskites containing $5d^1$ ions, such as Ba_2NaOsO_6,[1−5,8] Ba_2ZnReO_6[1,9] and Ba_2MgReO_6.[9−11] In all cases, experiments show that orbital order sets in at a higher temperature (T_o) than magnetic order (T_C). The magnetic structure is thought to be a noncollinear structure consisting of ferromagnetic layers, that are rotated/canted from one layer to the next. The canting angle between the Re^{6+}/Os^{7+} moments in neighboring layers, is sufficiently large (80−134°) that one can think of this

Received: July 30, 2024
Revised: November 14, 2024
Accepted: November 14, 2024
Published: November 28, 2024

noncollinear magnetic structure as being intermediate between collinear ferromagnetic and type I antiferromagnetic structures.[5,10] The Re/Os moments lie in the *ab* plane with no component along the *c*-axis. The saturation magnetization is found to be approximately 0.2−0.3 μ_B/f.u. In Ba_2MgReO_6, μSR studies[9] and resonant X-ray diffraction studies at the Re L_{III} absorption edge[11] both provide evidence of magnetic ordering below $T_C \approx 18$ K, but magnetic reflections have yet to been seen in neutron diffraction experiments.

Experimental studies of low temperature structural distortions in these phases are sparse. Hirai et al. have studied small single crystals of Ba_2MgReO_6 by synchrotron X-ray diffraction, where a subtle tetragonal distortion associated with orbital ordering was observed at 33 K.[11] Liu et al. have investigated the compound Ba_2NaOsO_6 using ^{23}Na-NMR.[5] In their study, local distortions around the Na^+ ions were observed, which imply distortions of the Os-centered octahedra, and are consistent with first-principles calculations.[12,13] Both studies see evidence for symmetry lowering, although a complete crystal structure of the low temperature phase has not been reported for either compound. That is to say, the space group and nature of the distortion were proposed, but occupied Wyckoff positions and atomic coordinates were not reported.

Prior studies raise several questions that this work seeks to address. Can these distortions be seen from diffraction measurements involving polycrystalline samples? What is the detailed crystal structure of the low temperature phase? Is there a magnetic dipole moment that can be detected with elastic neutron diffraction scattering techniques? If not, is the lack of a discernible moment due to instrumental limitations or a sign of multipolar order? Why does Ba_2LiOsO_6 adopt a different magnetic ground state than its closely related isoelectronic analogs? To answer these questions, we report here a detailed investigation of the symmetry breaking transitions (or lack thereof) in two double perovskites with a heavily canted antiferromagnetic ground state (Ba_2MgReO_6 and Ba_2ZnReO_6) and one with an antiferromagnetic ground state (Ba_2LiOsO_6). The results provide critical insight into the connections between orbital order, magnetic order, and structural distortions in these materials.

EXPERIMENTAL SECTION

Polycrystalline samples of Ba_2LiOsO_6, Ba_2ZnReO_6, and Ba_2MgReO_6 were prepared by solid-state methods. BaO (Sigma Alrich, 99.99% metals basis), Os powder (Sigma-Alrich, 99.9% trace metals basis), ReO_3 (Alfa Aesar, 99.9% trace metals basis), Re powder (Strem Chemicals, 99.9 9%), ZnO (Alfa Aesar, 99.99% metals basis), Li_2O (Alfa Aesar, 99.5%) were purchased from commercial sources and used as received. Stoichiometric amounts of the appropriate starting materials were thoroughly mixed using an agate mortar and pestle inside an argon filled glovebox. For the synthesis of Ba_2LiOsO_6, a separate alumina cap containing MnO_2 was also enclosed in the sealed quartz tube, as the decomposition of MnO_2 acts as the oxygen source needed to oxidize Os metal to Os^{7+} via the reaction $3\ MnO_2(s) \rightarrow Mn_3O_4(s) + O_2(g)$. The amount of MnO_2 used was sufficient to produce 1/4 mol excess $O_2(g)$ for every mole of double perovskite formed. For Ba_2LiOsO_6 and Ba_2ZnReO_6, each mixture was loaded into an alumina crucible and sealed in a silica tube under dynamic vacuum (~50 mTorr). Each tube was then placed in a furnace located inside a fume hood and heated to 1000 °C for 24−48 h with a heating rate of 1.5 °C/min and a cooling rate of 0.5 °C/min. The Ba_2MgReO_6 sample was prepared by conventional solid state synthesis routes in an argon atmosphere, as described previously.[9]

Powder X-ray diffraction (PXRD) data were collected on a Bruker D8 Advance powder diffractometer (40 kV, 40 mA, sealed Cu X-ray tube) equipped with a Lynxeye XE-T position-sensitive detector. The data were collected with an incident beam monochromator (Johansson type SiO_2-crystal) that selects only Cu Kα1 radiation (λ = 1.5406 Å). Synchrotron powder X-ray diffraction (PXRD) patterns were collected using the Oxford Helium Cryostat at the 11-BM beamline at the Advanced Photon Source at Argonne National Laboratory. Data were collected at select temperatures between 50 and 5.7 K for Ba_2LiOsO_6 and Ba_2ZnReO_6 over the angular range 5−55 2θ (λ = 0.460 Å). No sign of antisite disorder between the octahedral-site cations is seen. This is not surprising given the large difference in oxidation state between the diamagnetic cations (Li^+, Mg^{2+}, Zn^{2+}) and the $5d^1$ ions.

Time of flight neutron powder diffraction (TOF-NPD) was collected using the orange cryostat on the POWGEN beamline at the Spallation Neutron Source at Oak Ridge National Laboratory. Approximately 4 g of Ba_2LiOsO_6 and Ba_2ZnReO_6 were loaded into individual 6 mm vanadium cans. Data were collected at select temperatures between 50 and 1.7 K using Frame 1 (0.1−8 Å) and Frame 2 (0.5−12.5 Å). Constant wavelength neutron powder diffraction (CW-NPD) data were collected on Ba_2MgReO_6 using the high resolution D2B (λ = 1.594 Å) and the high intensity D20 (λ = 2.4178 Å) instruments at the Institute Laue-Langevin (ILL). The sample was loaded into a 12 mm cylindrical vanadium container and NPD measurements were performed at 1.5 and 30 K at D20, and subsequent measurements were conducted between 3.2 and 50 K at D2B to track the structural distortion in Ba_2MgReO_6. The counting times for each data set at D20 and D2B were 12 and 2 h, respectively. Rietveld refinements of both X-ray and neutron powder diffraction data were carried out using the TOPAS-Academic (Version 6) software package.[14] Images of the crystal structures were generated with VESTA 3.[15] Symmetry mode analysis was performed using ISODISTORT.[16,17]

Magnetic measurements were collected on a Quantum Design MPMS-3 SQUID magnetometer. Samples were prepared by filling a gel capsule with 90−100 mg of sample. The capsule was then mounted in a plastic straw. Temperature dependent magnetization under zero field-cooled (ZFC) and field-cooled (FC) conditions were collected from 2 to 300 K under an applied magnetic field of 1 kOe. Diamagnetic contributions were corrected using the constants described by Pascal.[18] Field dependent magnetization measurements were collected from −70 kOe to +70 kOe at 2 K. Magnetic measurements for Ba_2MgReO_6 can be found in reference[9].

^{7}Li (S = 3/2) nuclear magnetic resonance (NMR) measurements were performed at Brown University for magnetic fields up to 9 T and at the National High Magnetic Field Laboratory (NHMFL) in Tallahassee, FL at higher fields. In both laboratories high homogeneity superconducting magnets were used. The temperature control was provided by a ^{4}He variable temperature insert. The NMR data were recorded using a state-of-the art laboratory-made NMR spectrometer. The spectra were obtained, at each given value of the applied field, from the sum of spin−echo Fourier transforms recorded at constant frequency intervals. We used a standard spin−echo sequence ($\pi/2-\tau-\pi$). The shape of the spectra presented in the manuscript are independent of the duration of time interval τ. The ^{7}Li NMR measurements were taken on single crystals of Ba_2LiOsO_6. The mm sized single crystals were prepared by flux technique.[2] In a typical growth, 1 g of Ba_2LiOsO_6 powder, prepared by solid state reaction as described previously, was thoroughly mixed with reactive hydroxide flux. The homogeneous mixture was loaded into a Pt crucible covered with a Pt lid. The growth was performed inside of a box furnace. The mixture was first homogenized at 850 °C for 24 h, and then the furnace temperature was gradually reduced to 500 °C at a rate of 1 °C per hour. Afterward, the furnace was turned off. Millimeter-sized single crystals can be found at the bottom of the Pt crucible after the flux is washed away using methanol. Magnetic measurements confirm the antiferromagnetic ground state.

https://doi.org/10.1021/acs.chemmater.4c02135
Chem. Mater. 2024, 36, 11478−11489

RESULTS

Symmetry Mode Analysis. The ideal double perovskite structure adopts the form $A_2BB'O_6$ and consists of an infinite three-dimensional network of corner-connected $B(B')O_6$ octahedra, where the larger A-site cations sit in cuboctahedral cavities created by the network of corner-shared octahedra. In the ideal $Fm\bar{3}m$ structure there is only one oxygen position (24e) and the B/B′-cations sit in undistorted octahedra. Starting from the $Fm\bar{3}m$ parent space group, the introduction of the Γ_3^+ irrep allows the axial and equatorial oxygens to distort to give inequivalent bond distances in those directions, leading to two distinct oxygen sites (Wyckoff sites 4e and 8h). This distortion results in $I4/mmm$ space group symmetry (Figure 1a), which is rarely observed for double perovskites.[19]

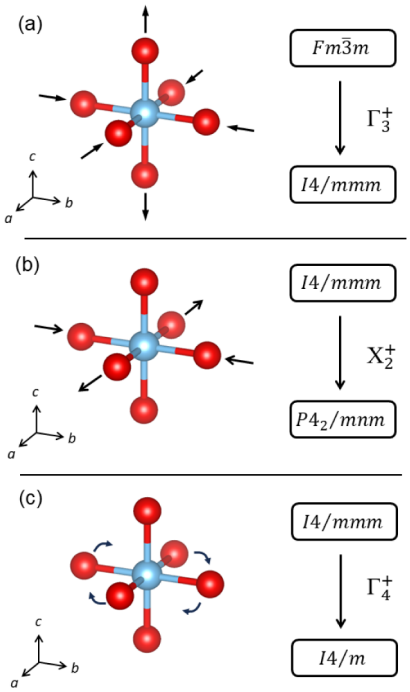

Figure 1. Symmetry mode analysis performed using $Fm\bar{3}m$ as the starting space group. The figure shows the distortions (parts a and b) and rotations (part c) of the octahedra containing the $5d^1$ ions. The octahedra containing diamagnetic ions are also allowed to distort (or rotate) but this is thought to be a response to the distortions of the octahedra containing $5d^1$ ions rather than a driver of the phase transition. The most common subgroups with their respective irreps and space group notation are highlighted. (a) The transformation from $Fm\bar{3}m$ to $I4/mmm$, (b) $I4/mmm$ to $P4_2/mnm$, and (c) $I4/mmm$ to $I4/m$.

Further addition of the X_2^+ irrep does not affect the oxygens in the axial position but causes an asymmetric distortion within the equatorial plane, leading to the formation of two distinct equatorial oxygens and three oxygen positions in total (Wyckoff sites 4e, 4f, and 4g) in the $P4_2/mnm$ space group (Figure 1b), which has been proposed as the low-temperature space group of Ba_2MgReO_6 and Ba_2NaOsO_6.[5,11] $I4/m$ is another common tetragonal space group adopted by double perovskite oxides such as Sr_2MReO_6 (M = Ni, Co, Zn).[20] The Γ_4^+ irrep introduces a rotation of the octahedra about the c axis (Figure 1c). The rotations occur in opposite directions from one layer to the next and are therefore referred to as out-of-phase rotations. In the notation originally proposed by Glazer this pattern of octahedral tilts/rotations is referred to as $a^0a^0c^-$.[21] Similar to the $I4/mmm$ structure there are two distinct oxygen positions. A summary of the symmetry mode analysis is shown in Figure 1.

Neutron powder diffraction has lower resolution than synchrotron PXRD. However, due to the weak X-ray scattering of oxygen atoms, NPD is the most suitable powder diffraction technique to accurately determine oxygen positions within the unit cell. From the symmetry analysis, the positions of the oxygen atoms along the ab plane are critical to distinguish between $I4/mmm$, $I4/m$ and $P4_2/mnm$ space groups and to explain the orbital ordering pattern that is thought to allow for stabilization of the heavily canted antiferromagnetic ground state reported for Ba_2MgReO_6, Ba_2ZnReO_6, and Ba_2NaOsO_6.

Ba_2LiOsO_6. In the ideal $Fm\bar{3}m$ space group, all Li ions sit at the center of a highly symmetric octahedron, leading to only one Li site. Experimentally, such a structure would produce a single peak in the ^{7}Li NMR spectrum. Ba_2LiOsO_6 is reported to order antiferromagnetically with a Néel temperature of 5.5 K, and our sample follows that behavior (Figure S1).[1,2,4] The antiferromagnetic ground state undergoes a spin flop transition to a ferromagnetic state in applied fields greater than 5.5 T.[4] Lithium-7 NMR data collected at both 3.3 and 13 T (Figure 2) show a single peak above and below the magnetic ordering temperature. The peak gets broader upon cooling, but no peak splitting is observed. Moreover, we observe more significant temperature dependence of the broadening in low fields where magnetic ground state is antiferromagnetic. These observations suggest no local symmetry breaking and that the Li-environment remains the same down to ≈2 K. These results are considerably different than those reported for Ba_2NaOsO_6,[5] where the single peak observed in the paramagnetic regime splits into two sets of triplets, signaling local symmetry breaking that leads to two different sites for the Na^+ ions. However, we cannot exclude the possibility that line width broadening observed at low temperatures in Ba_2LiOsO_6 masks very small local distortions. By taking into the account the value of the ^{7}Li quadrupolar moment relative to that of ^{23}Na, we can place an upper bound on the magnitude of the putative local symmetry breaking distortions. That is, we estimate that, at low field of 3.3. T, the magnitude of local distortions in Ba_2LiOsO_6 cannot exceed one-half of that observed in Ba_2NaOsO_6.[5]

Synchrotron PXRD diffraction patterns show no clear sign of peak splitting that would be indicative of a cubic-to-tetragonal transition down to 6 K (Figure 3a). TOF-NPD measurements collected at 20 and 1.7 K are indistinguishable, indicating that cubic $Fm\bar{3}m$ space group symmetry is maintained below T_N (Figure 3b). Furthermore, Rietveld refinements at 20 and 1.7 K (Table 1) using the four space groups discussed in the symmetry analysis show that at both temperatures, there is no significant improvement in the goodness of fit when using the $I4/mmm$ or $I4/m$ models. When using the $P4_2/mnm$ model, the R_{wp} actually increases by about 0.4%. In addition, all Os−O bond distances in the $I4/mmm$ and $I4/m$ models refine to the same value within the experimental uncertainty and the O−Os−O bond angles refine to values of 90° or 180°. Hence, the TOF-NPD is in agreement with the lack of peak splitting in synchrotron PXRD and corroborates the $Fm\bar{3}m$ space group assignment at both temperatures. Full details of the Rietveld refinements can be found in the Supporting Information (Tables S1 and S2).

https://doi.org/10.1021/acs.chemmater.4c02135
Chem. Mater. 2024, 36, 11478−11489

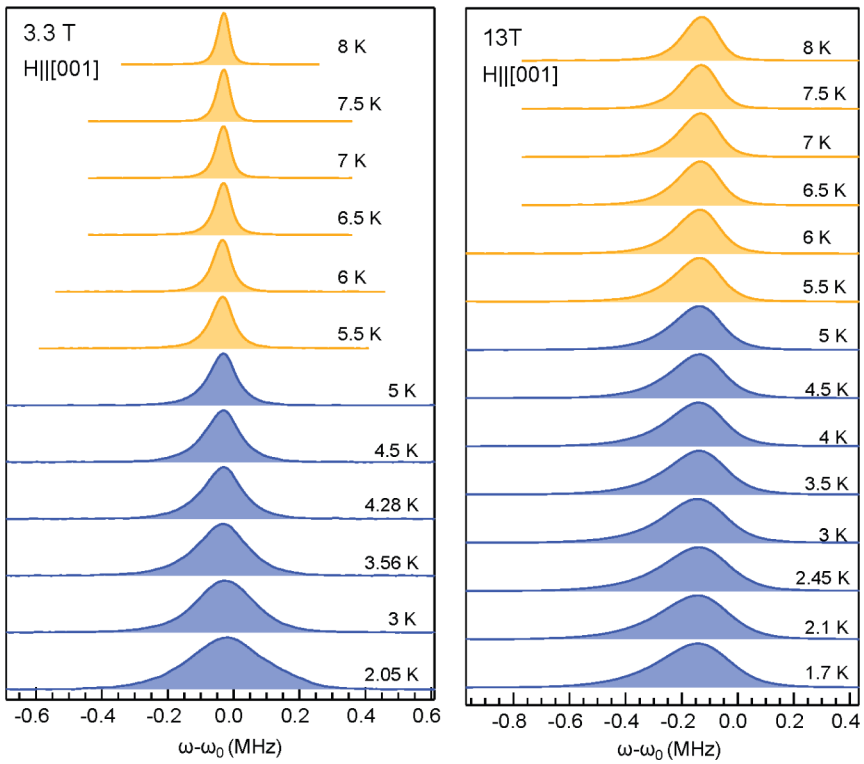

Figure 2. ^{7}Li NMR spectra taken on a sample of Ba_2LiOsO_6 in an applied field of 3.3 T, below the metamagnetic transition where the magnetic ground state is antiferromagnetic (left), and 13 T, where the magnetic ground state is ferromagnetic (right). Blue curves show the spectrum below magnetic transition and yellow curves above the magnetic transition. No quadrupolar splitting, indicative of a lowering of symmetry is observed in either case.

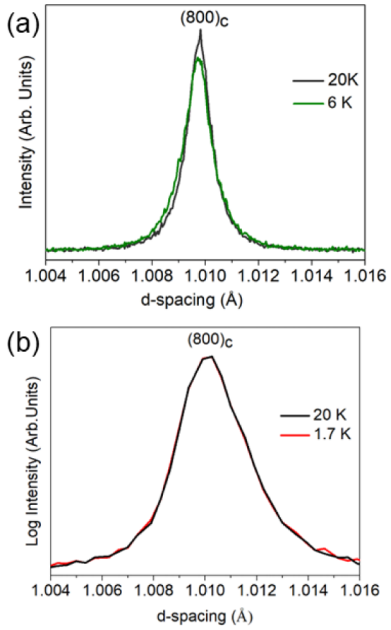

Figure 3. $(800)_{cub}$ peak of Ba_2LiOsO_6 as a function of temperature. (a) Synchrotron PXRD data at 20 K (black) and 6 K (green). (b) TOF-NPD data at 20 K (black) and 1.7 K (red).

Ba_2ZnReO_6. Variable-temperature high-resolution synchrotron PXRD data collected on Ba_2ZnReO_6 reveal a cubic-to-tetragonal structural transition upon cooling. The most evident feature of this distortion is the broadening and eventual splitting of various peaks, such as those corresponding to the cubic (00l) reflections. By inspecting the $c/\sqrt{2}a$ distortion parameter and the goodness of fit of the pattern using the cubic $Fm\bar{3}m$ model, we conclude that the tetragonal distortion starts at approximately 23 K (Figure 4). It should be noted that while one would expect the $c/\sqrt{2}a$ ratio to go to 1 in the cubic structure, the value tends to converge on a value slightly larger than 1 due to correlations in the refinement. For example, a $c/\sqrt{2}a$ of 1.0004 has previously been reported for Ba_2LiOsO_6 at 90 K, where there is no debate that the structure is cubic.[1] In Figure 4b, the $c/\sqrt{2}a$ stays constant at ≈1.0004 until around 23 K. Therefore, all the patterns collected above 23 K were fit with the cubic model. This assignment is also corroborated by a subtle feature at approximately 23 K observed in previously reported heat capacity data.[1] The structural transition temperature is higher than the magnetic transition temperature of 17 K (Figure S2). The observation of a structural transition occurring at a temperature higher than the onset of magnetic ordering has been previously reported for Ba_2MgReO_6, where the cubic-to-tetragonal distortion sets in at 33 K[11] and the magnetic transition occurs at 18 K.[9] The high-temperature structural transition has been attributed to orbital ordering (quadrupolar ordering in the J basis).[11] The degree of distortion ($c/\sqrt{2}a$) of 1.0014 observed for Ba_2ZnReO_6 at 6 K is comparable with the distortion of 1.0015 reported by Hirai et al. on Ba_2MgReO_6 single crystals at 6 K.[11] Values of the refined lattice constants are at each temperature are given in the Supporting Information (Table S3).

Due to the inherent lower resolution, the evidence of a tetragonal distortion is more difficult to see in the TOF-NPD data (Figure 5a) than in the synchrotron PXRD data. The broadening of the $(00l)_{cubic}$ reflections becomes more evident when comparing to the peaks that are not expected to split such as the $(222)_{cubic}$ (Figure 5b), which overlap completely at

https://doi.org/10.1021/acs.chemmater.4c02135
Chem. Mater. 2024, 36, 11478−11489

Table 1. Summary of Selected Rietveld Refinement Parameters of Ba_2LiOsO_6 as Obtained from Analysis of TOF-NPD Data at 20 and 1.7 K Using Various Structural Models[a]

	$Fm\bar{3}m$	$I4/mmm$	$P4_2/mnm$	$I4/m$
		Ba_2LiOsO_6 TOF-NPD 20 K		
R_{wp} (%)	5.467	5.465	5.878	5.452
a (Å)	8.07918(1)	5.71183(2)	5.71126(3)	5.71182(2)
c (Å)	N/A	8.08203(6)	8.0787(1)	8.08205(6)
Os−O axial (Å)	2 × 1.8948(4)	2 × 1.896(2)	2 × 1.907(5)	2 × 1.897(2)
Os−O eq 1 (Å)	2 × 1.8948(4)	2 × 1.892(1)	2 × 1.889(2)	2 × 1.892(5)
Os−O eq 2 (Å)	2 × 1.8948(4)	2 × 1.892(1)	2 × 1.889(2)	2 × 1.892(5)
		Ba_2LiOsO_6 TOF-NPD 1.7 K		
R_{wp} (%)	5.569	5.550	5.987	5.545
a (Å)	8.07911(1)	5.71173(2)	5.71114(4)	5.71179(2)
c (Å)	N/A	8.08206(6)	8.0788(1)	8.08197(6)
Os−O axial (Å)	2 × 1.8951(4)	2 × 1.895(2)	2 × 1.902 (5)	2 × 1.897(2)
Os−O eq 1(Å)	2 × 1.8951(4)	2 × 1.893(1)	2 × 1.891(2)	2 × 1.892(5)
Os−O eq 2 (Å)	2 × 1.8951(4)	2 × 1.893(1)	2 × 1.891(2)	2 × 1.892(5)

[a]The absence of any improvement in the fit when lowering the symmetry suggests that the cubic $Fm\bar{3}m$ is appropriate.

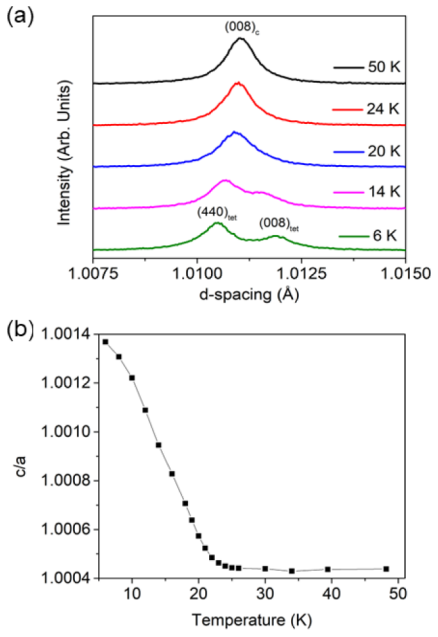

Figure 4. (a) Synchrotron PXRD data showing the evolution of the Ba_2ZnReO_6 $(008)_{cub}$ reflection as a function of temperature. At low temperature the splitting of this peak into the $(440)_{tet}$ and $(008)_{tet}$ reflections is evident. (b) Temperature dependence of the tetragonal distortion, $c/\sqrt{2}a$, obtained from Rietveld refinements of synchrotron PXRD data. The $I4/mmm$ space group was used to fit at all temperatures shown here.

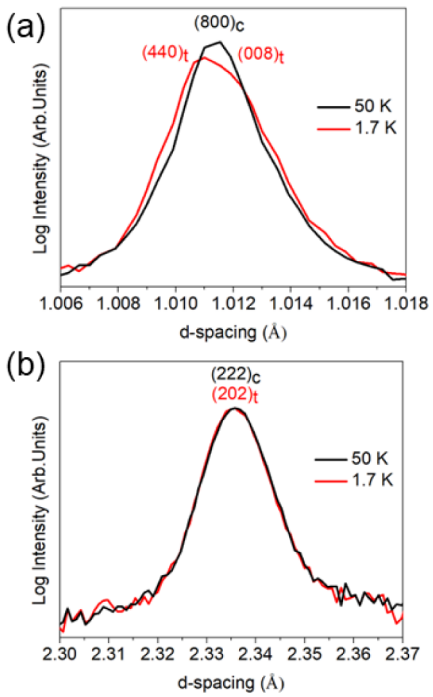

Figure 5. $(800)_{cub}$ and (b) $(444)_{cub}$ peak of Ba_2ZnReO_6 in TOF-NPD data at 50 K (black) and 1.7 K (red). The cubic to tetragonal distortion splits the $(800)_{cub}$ peak into the $(440)_{tet}$ and $(008)_{tet}$, but not the $(222)_{cub}$ peak, which becomes the $(202)_{tet}$ peak.

50 and 1.7 K. Despite the lower resolution, the higher sensitivity of NPD to the positions of the oxygen ions makes the TOF-NPD data better suited for accurate crystal structure determination. Table 2 summarizes the results of Rietveld refinements at 50 and 1.7 K using the cubic and tetragonal models proposed by the symmetry mode analysis previously discussed. At 50 K the pattern was successfully fit with the cubic model, and no significant improvement can be obtained with the various tetragonal models. At 1.7 K, the tetragonal space groups give a significantly better goodness of fit (R_{wp}). In addition, there is a clear elongation of the axial Re−O bond along the c-axis. Figure 6b shows that below orbital ordering temperature, the differences in axial and equatorial Re−O bond lengths are larger than the uncertainty in these values. These findings are supported by the synchrotron PXRD and heat capacity data, both of which indicate that the Ba_2ZnReO_6 undergoes a distortion when cooled below ≈23 K.

Among the tetragonal space groups suggested by the symmetry analysis, there was no improvement of the goodness of fit when reducing the symmetry from $I4/mmm$ to $P4_2/mnm$ or $I4/m$. In fact, the axial and equatorial Re−O bond distances refine to same values within error, independent of the space group. Furthermore, the Re−O−Re bond angles in the ab plane when using the $I4/m$ space group refined to 180°, which suggests that no tilting is present. For the $P4_2/mnm$ space group to produce a better fit, the equatorial oxygens should distort in opposite directions. However, the equatorial Re−O

https://doi.org/10.1021/acs.chemmater.4c02135
Chem. Mater. 2024, 36, 11478−11489

Table 2. Summary of Selected Rietveld Refinement Parameters of Ba_2ZnReO_6 TOF-NPD Data at 50 K and 1.7K Using the Following Space Groups: $Fm\bar{3}m$, $I4/mmm$, $P4_2/mnm$, and $I4/m$

Space group	$Fm\bar{3}m$	$I4/mmm$	$P4_2/mnm$	$I4/m$
		Ba_2ZnReO_6 TOF-NPD 50 K		
R_{wp} (%)	11.536	11.472	11.393	11.466
a (Å)	8.08972(3)	5.71922(6)	5.7275(2)	5.71925(6)
c (Å)	N/A	8.0927(3)	8.1023(4)	8.0927(2)
Re−O axial (Å)	2 × 1.9228(6)	2 × 1.926(4)	2 × 1.925(6)	2 × 1.927(5)
Re−O eq 1 (Å)	2 × 1.9228(6)	2 × 1.922(3)	2 × 1.923(4)	2 × 1.922(4)
Re−O eq 2 (Å)	2 × 1.9228(6)	2 × 1.922(3)	2 × 1.923(4)	2 × 1.922(4)
		Ba_2ZnReO_6 TOF-NPD 1.7 K		
R_{wp} (%)	12.774	11.237	11.897	11.521
a (Å)	8.08909(4)	5.71743 (3)	5.71747(4)	5.71742(4)
c (Å)	N/A	8.09620(9)	8.0960(1)	8.09620(9)
Re−O axial (Å)	2 × 1.9223(7)	2 × 1.930(2)	2 × 1.931(5)	2 × 1.930(2)
Re−O eq 1 (Å)	2 × 1.9223(7)	2 × 1.919(1)	2 × 1.92(5)	2 × 1.921(3)
Re−O eq 2 (Å)	2 × 1.9223(7)	2 × 1.919(1)	2 × 1.92(5)	2 × 1.921(3)

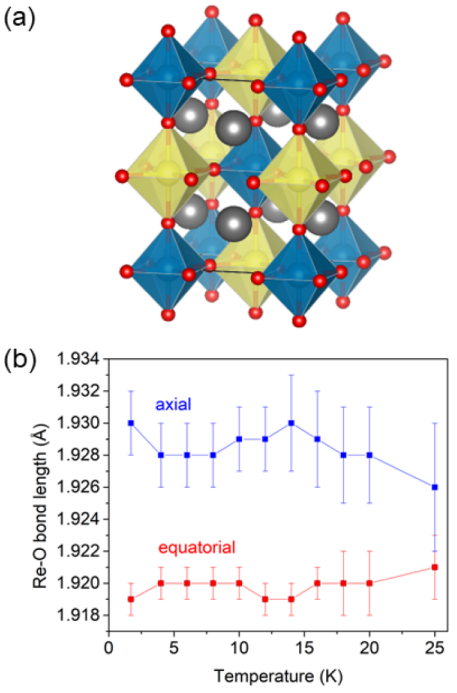

Figure 6. (a) The structure of Ba_2ZnReO_6 with $I4/mmm$ symmetry as determined from the TOF-NPD data at 1.7 K. (b) The Re−O bond distances as a function of temperature as determined from TOF-NPD data.

bond distances in this space group refined to the same value, with rather large uncertainties. Therefore, we find no compelling experimental evidence in the *powder diffraction data* to justify lowering the symmetry from $I4/mmm$ (Figure 6a). Full refinement results can be found in the Supporting Information (Tables S4 and S5).

Ba_2MgReO_6. A detailed study on Ba_2MgReO_6 single crystals has been conducted by Hirai et al. and from that study it was concluded that orbital ordering (quadrupolar ordering) occurs at T_0 = 33 K followed by long-range magnetic ordering at T_C = 18 K.[10,11] It was also concluded that the space group symmetry was lowered from $Fm\bar{3}m$ to $P4_2/mnm$.[11] We reinvestigated this compound using polycrystalline samples to determine if the same types of distortions could be detected using NPD.

Variable temperature CW-NPD data collected for Ba_2MgReO_6 shows clear broadening/splitting of a few cubic reflections, such as the (008), upon cooling (Figure 7a). The

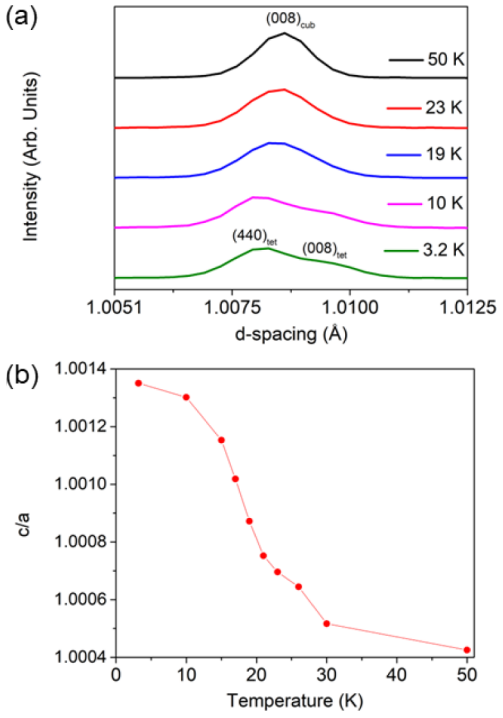

Figure 7. (a) Constant wavelength NPD data showing the evolution of the Ba_2MgReO_6 $(008)_{cub}$ reflection as a function of temperature. At low temperature the splitting of this peak into the $(440)_{tet}$ and $(008)_{tet}$ reflections is evident. (b) Temperature dependence of the tetragonal distortion, $c/\sqrt{2}a$, obtained from Rietveld refinements of constant wavelength NPD data. The $I4/mmm$ space group was used to fit at all temperatures shown here.

$c/\sqrt{2}a$ value at 3.2 K of 1.0014 (Figure 7b) matches the value obtained for the Ba_2ZnReO_6 sample and is in close agreement with the value of 1.0015 reported by Hirai et al. on Ba_2MgReO_6 single crystals.[11] Lattice parameters obtained at each temperature are given in the Supporting Information (Table S6). Fits with the four different space groups proposed by the symmetry analysis were also performed with the data sets obtained at 50 and 3.2 K (Tables 3, S7, and S8). At 50 K,

https://doi.org/10.1021/acs.chemmater.4c02135
Chem. Mater. 2024, 36, 11478−11489

Table 3. Summary of Selected Rietveld Refinement Parameters of Ba_2MgReO_6 CW-NPD data at 50 and 3.2 K Using the Following Space Groups: $Fm\bar{3}m$, $I4/mmm$, $P4_2/mnm$, and $I4/m$

Space group	$Fm\bar{3}m$	$I4/mmm$	$P4_2/mnm$	$I4/m$
		Ba_2MgReO_6 CW-NPD 50 K		
R_{wp} (%)	6.916	7.044	7.041	7.039
a (Å)	8.06970(2)	5.70541(4)	5.70539(4)	5.70542(4)
c (Å)	N/A	8.0721(1)	8.0721(1)	8.0721(1)
Re−O axial (Å)	2 × 1.923(1)	2 × 1.918(6)	2 × 1.920(6)	2 × 1.919(6)
Re−O eq 1 (Å)	2 × 1.923(1)	2 × 1.924(3)	2 × 1.92(4)	2 × 1.926(8)
Re−O eq 2 (Å)	2 × 1.923(1)	2 × 1.924(3)	2 × 1.93(4)	2 × 1.926(8)
		Ba_2MgReO_6 CW-NPD 3.2 K		
R_{wp} (%)	9.195	7.031	7.101	7.029
a (Å)	8.06915(4)	5.70331(2)	5.70335(2)	5.70330(2)
c (Å)	N/A	8.07659(6)	8.07666(6)	8.07658(6)
Re−O axial (Å)	2 × 1.922(1)	2 × 1.926(3)	2 × 1.928(2)	2 × 1.925(3)
Re−O eq 1 (Å)	2 × 1.922(1)	2 × 1.920(1)	2 × 1.91(2)	2 × 1.922(6)
Re−O eq 2 (Å)	2 × 1.922(1)	2 × 1.920(1)	2 × 1.92(2)	2 × 1.922(6)

no sign of peak broadening/splitting was observed and the R_{wp} of the cubic model was slightly lower than the tetragonal models, confirming the $Fm\bar{3}m$ space group assignment. This assignment agrees with the heat capacity and the previously reported single crystal data.[10,11] At 3.2 K, clear peak splitting, such as observed for the (008) cubic peak, reveals the tetragonal distortion. This conclusion is further supported by an improvement of over 2% in the goodness of fit obtained in Rietveld refinements using the tetragonal models over the cubic model. When looking at the three possible tetragonal models, one can observe that the $P4_2/mnm$ space group produces Re−O equatorial bonds with larger esds than the other models. In addition, the three tetragonal models produced the same Re−O bond distances within error and very similar goodness of fit. Therefore, we opted to use the $I4/mmm$ model (Table S8) as it produces meaningful Re−O bond distances and has the fewest variables. Detailed variable temperature analysis considering the goodness of fit, fwhm, and Re−O bond distances shows that the cubic-to-tetragonal transition becomes apparent below the previously reported orbital ordering temperature (33 K), but above the magnetic ordering temperature (18 K) in agreement with previous studies.[9−11]

Neutrons are ideally suited to probe long-range ordering of magnetic dipole moments. Hirai et al. have proposed a magnetic structure for Ba_2MgReO_6 based on resonant X-ray scattering results.[11] The k-vector is identified as [0 0 1] and thus, there are only two magnetic sites per cell, the Re ions at (0 0 0) and at (1/2 1/2 1/2). The model consists of ferromagnetic layers with a rather large canting angle of ≈80° between the Re moments in each layer (Figure 8a). The Re moments lie in the ab plane with no z component. Bulk magnetic measurements on Ba_2MgReO_6 from several sources on both powders—including the same sample measured in this work[9] —and single crystals[11] have shown ferromagnetic-like behavior below 19 K with a saturation moment of ≈0.3 μ_B. This moment is also comparable to the ones obtained for Ba_2ZnReO_6.[1] In the single crystal data for Ba_2MgReO_6 the moment is oriented along [100] in the tetragonal cell. With these constraints, one can deduce an expected ordered Re moment of ≈0.4 μ_B as shown in Figure 8b. While this is a relatively small moment, if it is primarily dipolar in origin, it should be detectable with high intensity neutron data.

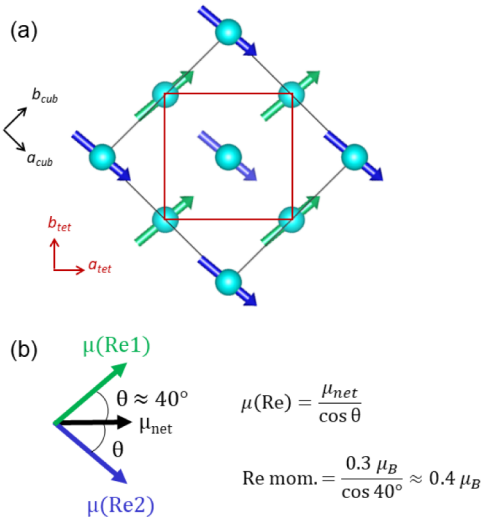

Figure 8. (a) The magnetic structure of Ba_2MgReO_6 proposed by Hirai et al.[11] Purple moments belong to rhenium ions in the plane with $z = 0$, and green moments to the rhenium ions in the plane with $z = 1/2$. The cubic unit cell is shown in black and the tetragonal unit cell in red. (b) The relationship between the individual rhenium moments, μ(Re1) and μ(Re2) and the net moment per rhenium, μ_{net}, oriented along the $[100]_{tet}$ or the $[110]_{cub}$ direction.

To this end, CW-NPD data were collected using the high intensity instrument D20 at 1.5 and 30 K and a wavelength of 2.4178 Å. Figure S3 shows both data sets in the low Q region where magnetic reflections of dipolar origin would be expected. Clearly, the two are nearly superimposed with no obvious differences. In Figure 9, the 30 K data are subtracted from the 1.5 K in an attempt to observe any magnetic reflections. There is no indication of the (100) reflection seen in the earlier resonant X-ray study.[11] A simulation with Re moments of 0.4 μ_B resulted in a (001) reflection which was more intense than the noise in the pattern by a factor of ∼16. This clearly shows that the magnetic structure is more complicated than the one assumed in the literature and shown in Figure 8. If there is a magnetic dipole component associated with the Re moment, it is no larger than 0.1 μ_B (Figure S4) and therefore significantly smaller than the multipolar component. It is worth noting that small dipolar ordered moments of magnitude 0.3 μ_B have been detected

https://doi.org/10.1021/acs.chemmater.4c02135
Chem. Mater. 2024, 36, 11478−11489

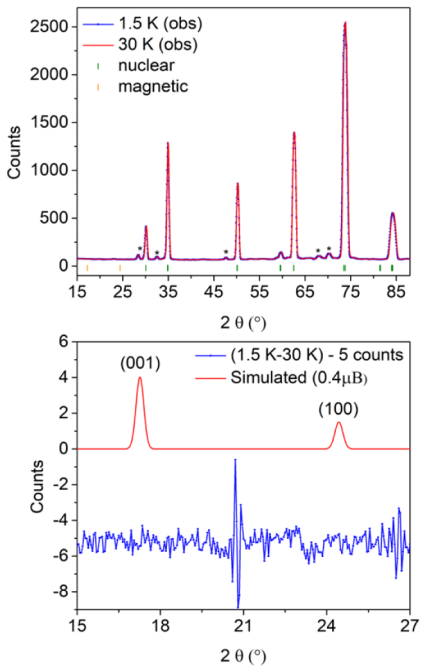

Figure 9. Upper image shows neutron powder diffraction patterns of Ba_2MgReO_6 collected at the high intensity D20 beamline at temperatures above (30 K) and below (1.5 K) the magnetic ordering temperature. The peaks marked with an asterisk from an unknown secondary phase and are not indexed, but present at all temperatures. The lower image shows a calculated pattern of the two strongest magnetic peaks for the heavily canted antiferromagnetic structure shown in Figure 8 and a moment of 0.4 μ_B per Re (in red) plotted against a plot of the 1.5 K data minus the 30 K data.

using neutron diffraction for related double perovskites, such as La_2LiMoO_6 ($4d^1$),[22] Ba_2YReO_6 ($5d^2$),[23] and Ba_2LuReO_6 ($5d^2$).[24] These are among the smallest ordered dipolar moments detected among the double perovskite family of materials. Clearly any dipole moment in Ba_2MgReO_6 is smaller than these examples, which would suggest multipolar ordering. It is now well established that neutron scattering from magnetic octupolar moments can only be seen at much higher Q than the studies reported here.[25,26] Future searches using neutron diffraction to find evidence for multipolar order in Ba_2MgReO_6 should be optimized accordingly.

DISCUSSION

Most double perovskites that contain a $5d^1$ ion and possess a cubic structure at room temperature display hysteresis loops and a saturated moment that is consistent with a heavily canted antiferromagnetic ground state, including Ba_2NaOsO_6,[1−4] Ba_2MgReO_6,[9−11] and Ba_2ZnReO_6.[1,9] An intriguing exception is Ba_2LiOsO_6, which adopts an antiferromagnetic ground state.[1,2,4] The data presented here show that Ba_2LiOsO_6 deviates from the other compounds in another important way. It retains cubic symmetry and ideal octahedral site symmetry about the $5d^1$ ion, down to at least 2 K. In contrast, we observe a cubic-to-tetragonal distortion in Ba_2ZnReO_6 and Ba_2MgReO_6 at temperatures of approximately 23 and 33 K, respectively. In both compounds these transitions occur at temperatures that are unambiguously higher than the onset of long-range magnetic ordering. The behavior of Ba_2LiOsO_6 is also unlike Ba_2NaOsO_6, where previous NMR studies showed symmetry lowering that breaks the local octahedral symmetry below 13 K.[5] Furthermore, the electric field gradient seen at the Na nucleus is in good agreement with the three inequivalent Os−O distances expected for the $P4_2/mnm$ low-temperature structure. This type of distortion is consistent with the pattern of orbital ordering, driven by Coulombic repulsions, predicted by theoretical and computational modeling to stabilize the heavily canted antiferromagnetic ground state.[6,7,27]

The agreement with theory is less direct when we consider the symmetry of the low temperature tetragonal structure seen here for Ba_2ZnReO_6 and Ba_2MgReO_6. Below the orbital ordering temperature, synchrotron PXRD, TOF-NPD and CW-NPD for both compounds can be successfully fit with the $I4/mmm$ space group and provide no clear experimental evidence to favor the $P4_2/mnm$ structure. From the symmetry analysis, the introduction of the X_2^+ irrep allows an asymmetric displacement of the equatorial oxygens that changes the lattice centering from body-centered to primitive. Such a distortion reduces the number of systematic absences and in principle leads to the appearance of reflections where $h + k + l \neq 2n$, such as (416), (434), (335) and (513). Reflections of this type are not observed in the NPD patterns of either Ba_2ZnReO_6 or Ba_2MgReO_6. However, in the Ba_2MgReO_6 single crystal study, 141 reflections that violate the systematic absences of the $I4/mmm$ space group were observed below the orbital ordering temperature.[11] These reflections are reported to be very weak, with intensities corresponding to less than 0.005% of the strongest reflection in the pattern, which raises the possibility that they are too weak to be seen in the powder diffraction data reported here.

To explore this possibility, we have simulated NPD patterns using the instrumental parameters of both TOF-NPD and CW-NPD (Figure 10). The positions of the equatorial oxygen atoms in the $P4_2/mnm$ space group are described as following: $(x - \delta x, x - \delta x, 0)$ and $(x + \delta x, -x - \delta x, 0)$, where δx is fractional coordinate displacement of the oxygen atoms along the ab plane. For the simulations, neutron diffraction patterns were calculated corresponding to (1) $\delta x = 0$, which would correspond to the $I4/mmm$ structure; (2) $\delta x = 0.00277$, that matches the distortion observed by Hirai et al.[11] and obtained in calculations performed by Tehrani and Spaldin,[27] which results in Re−O_{eq} bonds that differ by ≈0.04 Å; and (3) $\delta x = 0.00831$, a distortion that would result in Re−O_{eq} bonds that differ by ≈0.13 Å (Tables S9 and S10). From the simulated patterns shown in Figure 10, it is possible to conclude that the extra reflections that are allowed in the $P4_2/mnm$ structure, but forbidden in the $I4/mmm$ structure, would be extremely weak and below the detection limit of both instruments used in this study, if the predicted distortion (δx) matches previous reports ($\delta x = 0.00277$). However, if the distortion was three times larger than previously reported ($\delta x = 0.00831$), the superlattice reflections would be visible in our NPD patterns. Based on this analysis we conclude that powder diffraction techniques can detect the cubic-to-tetragonal distortion, but are not capable of detecting the subtle distortion caused by the displacement oxygen atoms that differentiate the $I4/mmm$ and $P4_2/mnm$ tetragonal models. To detect such peaks an instrument with exceptionally low background counts and a better signal-to-noise ratio would be required.

It is surprising that Ba_2LiOsO_6 behaves differently than from its isoelectronic and isostructural (at room temperature) counterparts Ba_2ZnReO_6 and Ba_2MgReO_6. The divergent behavior is particularly intriguing given the similar unit cell

https://doi.org/10.1021/acs.chemmater.4c02135
Chem. Mater. 2024, 36, 11478−11489

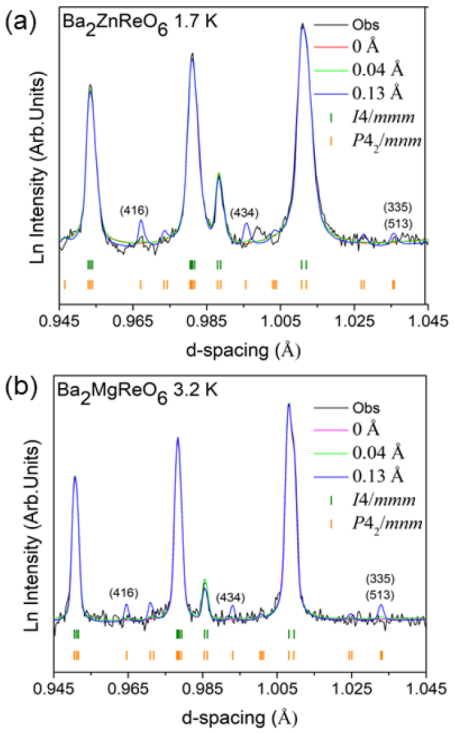

Figure 10. Observed and simulated NPD patterns for (a) Ba_2ZnReO_6 (b) Ba_2MgReO_6. The pink curve is simulated from the refined structure with $I4/mmm$ symmetry, the blue and green curves are simulated from hypothetical structures with $P4_2/mnm$ space group symmetry. The latter two differ from one another in the magnitude of the distortion parameter δx, as explained in the text. Green and orange tick marks correspond to the allowed peak positions for the $I4/mmm$ and $P4_2/mnm$ space groups, respectively. The Miller indices shown correspond to peaks that are allowed for $P4_2/mnm$ but absent for $I4/mmm$.

dimensions and distances between magnetic ions summarized in Table 4. Theoretical modeling of double perovskites containing $5d^1$ ions predict phase diagrams with closely competing magnetic ground states.[6,7] The balance between these states depends on variables that include the Coulomb repulsion between the magnetic ions (V), the strength of the superexchange interactions (J_{SE}), the magnitude of spin−orbit coupling (λ), Hund's coupling (J_H), and Hubbard U. Recent high-pressure studies of Ba_2MgReO_6 show that at pressures greater than ∼5 GPa the quadrupolar charge ordering is suppressed and the heavily canted antiferromagnetic state gives way to a collinear antiferromagnetic state.[28] This study illustrates how delicate the balance is between competing ground states.

Table 4. Characteristic Features of Double Perovskites Studied in This Work

	Ba_2MgReO_6	Ba_2LiOsO_6	Ba_2ZnReO_6
	Phase Transitions		
orbital ordering, T_0	33 K	none	23 K
magnetic ordering	Canted AFM (T_C = 18 K)	AFM (T_N = 5.5 K)	Canted AFM (T_C = 16 K)
	Structure at Room Temperature[a]		
space group	$Fm\bar{3}m$	$Fm\bar{3}m$	$Fm\bar{3}m$
unit cell volume/ formula unit	132.1 Å	132.9 Å^3	133.2 Å^3
Re(Os)−Re(Os) distance (Å)	5.717 Å	5.729 Å	5.732 Å
	Structure at T < 4 K		
space group	$P4_2/mnm$ or $I4/mmm$	$Fm\bar{3}m$	$P4_2/mnm$ or $I4/mmm$
unit cell volume/ formula unit	131.4 Å^3	131.8 Å^3	132.3 Å^3
Re(Os)−Re(Os) distance	5.703 Å, 5.707 Å	5.713 Å	5.717 Å, 5.721 Å

[a]Room temperature structural data taken from reference[1] for Ba_2LiOsO_6 and Ba_2ZnReO_6, and from reference[9] for Ba_2MgReO_6.

As shown in Table 4, the details of the host structure above T_o are effectively the same for Ba_2LiOsO_6, Ba_2ZnReO_6, and Ba_2MgReO_6, so the different behavior of Ba_2LiOsO_6 at low temperature must arise from the subtle differences between the 5d ions themselves. Since the distances between magnetic centers are nearly identical for all three compounds, one would naively think that the higher oxidation state of osmium (Os^{7+} vs Re^{6+}) would lead to a higher Coulomb repulsion V between transition metal ions. However, this cannot explain the antiferromagnetism of Ba_2LiOsO_6, as the theoretical modeling indicates that a larger V favors the heavily canted antiferromagnetic state. The phase diagram given in reference[7] provides another pathway to stabilization of an antiferromagnetic ground state, namely by decreasing J_{SE}/λ. The higher oxidation state of osmium should lead to slightly higher covalency with oxygen, and naively one would expect that to enhance the superexchange coupling J_{SE}, though the effect could be small. On the other hand, the free ion spin−orbit coupling constant for Os^{7+} (and λ = 640 meV) is nearly 20% larger than that of Re^{6+} (λ = 540 meV).[29] This increase in λ could lead to a decrease in J_{SE}/λ that is large enough to stabilize the antiferromagnetic ground state in Ba_2LiOsO_6. It is also worth noting that while Ba_2LiOsO_6 undergoes a spin flip transition to a ferromagnetic state in magnetic fields greater than 5.5 T, the ^{7}Li NMR results presented here show that in the field-stabilized ferromagnetic state the structural distortion seen in Ba_2MgReO_6, Ba_2ZnReO_6, and Ba_2NaOsO_6 is not observed.

Using a local dipole moment of ≈0.4 μ_B/Re, estimated from magnetization measurements on Ba_2ZnReO_6 and Ba_2MgReO_6, we were able to simulate the expected magnetic reflections that would result from ordering of conventional dipolar moments. While the reflections are weak (the (001) peak is predicted to be ∼0.1% as intense as the strongest nuclear reflection), if Ba_2MgReO_6 underwent conventional ordering of dipolar magnetic moments, it should be possible to see some intensity for the (001) magnetic reflection using the high intensity D20 diffractometer. From the lack of observed magnetic scattering, we estimate an upper limit of 0.1 μ_B for the dipolar contribution to the magnetic moment. This moment would not be large enough to explain the saturation magnetization seen in magnetometry. Lovesey and Khalyavin have considered the interaction between magnetic dipoles and the electric quadrupoles created when Ba_2MgReO_6 undergoes orbital ordering.[30] At low angles (high d-spacing), where dipolar magnetic scattering is strongest, neutron scattering from magnetic multipoles is vanishingly small. On the other hand, the intensities for resonant X-ray scattering are different, which may help to explain why Hirai et al. were able to observe the (001) peak.[11]

The local moments in the magnetically ordered state cannot be purely quadrupolar in nature, because quadrupolar ordering does not break time reversal symmetry and therefore cannot be

https://doi.org/10.1021/acs.chemmater.4c02135
Chem. Mater. 2024, 36, 11478−11489

responsible for the bulk magnetization of the sample. On the other hand, ferromagnetic (or perhaps heavily canted antiferromagnetic) ordering of octupoles could explain the lack of detectable magnetic reflections and the bulk magnetization of these samples. The magnetism of Ba_2MgReO_6 and Ba_2ZnReO_6 would appear to have parallels with NpO_2. Magnetic susceptibility measurements of NpO_2 show Curie–Weiss behavior with an effective moment of 2.95 μ_B per Np^{4+} ion and apparent antiferromagnetic ordering at 25 K.[31] Specific heat, μSR, Mössbauer, and resonant X-ray scattering studies all find evidence of antiferromagnetic ordering.[32−34] Yet multiple neutron diffraction studies have yet to find any sign of magnetic reflections.[35,36] The difficulty in seeing signs of magnetic scattering of neutrons is thought be a sign of magnetic octupoles, and it is possible that the same considerations apply to double perovskites like Ba_2MgReO_6 and Ba_2ZnReO_6, where the effective moment is considerably smaller than it is in NpO_2.

The final point to be made is that double perovskites containing $5d^1$ ions are not a monolith. The compounds studied here all have tolerance factors (t) substantially larger than one—Ba_2MgReO_6 (t = 1.054), Ba_2LiOsO_6 (t = 1.050), and Ba_2ZnReO_6 (t = 1.049). The large tolerance factor inhibits octahedral tilting distortions that typically lead to a transition from cubic $Fm\bar{3}m$ to tetragonal $I4/m$.[37,38] When the tolerance factor decreases, as it does for Ba_2CaReO_6 (t = 0.985) and Ba_2CdReO_6 (t = 0.997), $Fm\bar{3}m$ to $I4/m$ transitions typically occur upon cooling. These phase transitions, which occur at ≈130 K for Ba_2CaReO_6 and ≈170 K for Ba_2CdReO_6, are associated with out-of-phase tilting of octahedra and are presumably driven by Ba−O ionic bonding.[1,39,40] In Sr_2MgReO_6 (t = 0.994) the $I4/m$ structure is stabilized to some unknown temperature above room temperature.[41,42] As shown in Figure 1, the distortion of the octahedra containing the $5d^1$ ion is different in compounds with $I4/m$ symmetry than it is in compounds with $P4_2/mnm$ symmetry. This appears to alter the orbital occupation in such a way so as to favor a collinear antiferromagnetic structure in Ba_2CaReO_6 (T_N = 16 K),[39] Ba_2CdReO_6 (T_N = 4 K),[1] and Sr_2MgReO_6 (T_N = 55 K).[41] Even in these compounds the magnetic ground state appears to be sensitive to subtle changes in composition or defects, as Ba_2CdReO_6 has also been reported to adopt a heavily canted antiferromagnetic ground state[40] and Sr_2MgReO_6 a spin-glass type ground state.[42]

CONCLUSION

A comprehensive study using high resolution synchrotron and neutron powder diffraction techniques together with ^{7}Li NMR, has been conducted to explore the links between crystal structure, orbital ordering, and magnetism in three different double perovskite compositions containing ions with a $5d^1$ electron configuration. In Ba_2ZnReO_6 a cubic-to-tetragonal transition occurs at 23 K that breaks the degeneracy of the t_{2g} orbitals and presumably leads to a pattern of orbital ordering that stabilizes magnetic ordering at 16 K. Similar transitions occur in Ba_2MgReO_6 at 33 and 18 K. Unfortunately, powder diffraction methods are not sensitive enough to differentiate between the $I4/mmm$ and $P4_2/mnm$ structural models. Both diffraction measurements and ^{7}Li NMR data show that Ba_2LiOsO_6 retains a cubic structure down to 1.7 K. The antiferromagnetic ground state and lack of a structural distortion in Ba_2LiOsO_6, show that the tetragonal distortion seen in Ba_2ZnReO_6 and Ba_2MgReO_6, is intimately linked to the quadrupolar ordering and the ferromagnetic-like magnetism seen in those compounds at lower temperatures. Finally, no sign of magnetic scattering can be detected in high intensity NPD patterns collected on Ba_2MgReO_6, which strongly suggests long-range ordering of magnetic octupoles.

ASSOCIATED CONTENT

Supporting Information

The Supporting Information is available free of charge at https://pubs.acs.org/doi/10.1021/acs.chemmater.4c02135.

Magnetization measurements on Ba_2LiOsO_6 (Figure S1); magnetization measurements on Ba_2ZnReO_6 (Figure S2); details of Rietveld refinements of the crystal structures of Ba_2LiOsO_6 (Tables S1, S2), Ba_2ZnReO_6 (Tables S3, S4, S5), and Ba_2MgReO_6 (Tables S6, S7, S8); bond distances associated with various degrees of distortion for the low temperature $P4_2/mnm$ structure (Tables S9, S10); high intensity NPD data of Ba_2MgReO_6 collected on beamline D20 (Figures S3, S4) (PDF)

Crystallographic data of Ba_2LiOsO_6 at 20 K (CIF)

Crystallographic data of Ba_2LiOsO_6 at 1.7 K (CIF)

Crystallographic data of Ba_2ZnReO_6 at 50 K (CIF)

Crystallographic data of Ba_2ZnReO_6 at 1.7 K (CIF)

Crystallographic data of Ba_2MgReO_6 at 50 K (CIF)

Crystallographic data of Ba_2MgReO_6 at 3.2 K (CIF)

AUTHOR INFORMATION

Corresponding Author

Patrick M. Woodward − *Department of Chemistry and Biochemistry, The Ohio State University, Columbus, Ohio 43210, United States;* orcid.org/0000-0002-3441-2148; Email: woodward.55@osu.edu

Authors

Victor da Cruz Pinha Barbosa − *Department of Chemistry and Biochemistry, The Ohio State University, Columbus, Ohio 43210, United States*

Dalini D. Maharaj − *Department of Physics and Astronomy, McMaster University, Hamilton, Ontario L8S 4M1, Canada*

Zachery W. Cronkright − *Department of Chemistry, McMaster University, Hamilton, Ontario L8S 4M1, Canada*

Ye Wang − *Department of Chemistry and Biochemistry, The Ohio State University, Columbus, Ohio 43210, United States*

Rong Cong − *Department of Physics, Brown University, Providence, Rhode Island 02912, United States; National High Magnetic Field Laboratory, Florida State University, Tallahassee, Florida 32310, United States*

Erick Garcia − *Department of Physics, Brown University, Providence, Rhode Island 02912, United States*

Arneil P. Reyes − *National High Magnetic Field Laboratory, Florida State University, Tallahassee, Florida 32310, United States*

Jiaqiang Yan − *Materials Science and Technology Division, Oak Ridge National Laboratory, Oak Ridge, Tennessee 37831, United States;* orcid.org/0000-0001-6625-4706

Clemens Ritter − *Institute Laue Langevin, F-38042 Grenoble, France*

Vesna F. Mitrović − *Department of Physics, Brown University, Providence, Rhode Island 02912, United States*

Bruce D. Gaulin − *Department of Physics and Astronomy, McMaster University, Hamilton, Ontario L8S 4M1, Canada*

John E. Greedan − *Department of Chemistry, McMaster University, Hamilton, Ontario L8S 4M1, Canada;* orcid.org/0000-0003-1307-8379

Complete contact information is available at: https://pubs.acs.org/10.1021/acs.chemmater.4c02135

Notes

The authors declare no competing financial interest.

■ ACKNOWLEDGMENTS

This work is dedicated to Professor Francis DiSalvo who is fondly remembered for his unbounded enthusiasm and numerous contributions to the field of solid state chemistry. V.P.B., Y.W., and P.M.W. acknowledge support from the Center for Emergent Materials, an NSF MRSEC, under Award DMR-2011876. Use of the Advanced Photon Source at Argonne National Laboratory was supported by the U.S. Department of Energy, Office of Science, Office of Basic Energy Sciences, under Contract No. DE-AC02-06CH11357. V.F.M. acknowledges the support from the by U.S. National Science Foundation (NSF) Grant No. DMR-1905532. The NMR study at the NHMFL was supported by the National Science Foundation under Cooperative Agreement no. DMR-1644779 and the State of Florida. J.Q.Y. was supported by the US Department of Energy, Office of Science, Basic Energy Sciences, Materials Sciences and Engineering Division. A portion of this research used resources at the Spallation Neutron Source, a DOE Office of Science User Facility operated by the Oak Ridge National Laboratory. The authors thankfully acknowledge Qiang Zhang and Melanie Kirkham for experimental assistance with POWGEN data collection. The ILL is acknowledged for beam time allocation under the experiment code 5-31-2577. Finally, we acknowledge Mohit Randeria for insightful conversations.

■ REFERENCES

(1) da Cruz Pinha Barbosa, V.; Xiong, J.; Tran, P. M.; McGuire, M. A.; Yan, J.; Warren, M. T.; Aguilar, R. V.; Zhang, W.; Randeria, M.; Trivedi, N.; Haskel, D.; Woodward, P. M. The Impact of Structural Distortions on the Magnetism of Double Perovskites Containing $5d^1$ Transition-Metal Ions. *Chem. Mater.* **2022**, *34*, 1098−1109.

(2) Stitzer, K. E.; Smith, M. D.; Zur Loye, H. C. Crystal growth of Ba_2MOsO_6 (M = Li, Na) from reactive hydroxide fluxes. *Solid State Sci.* **2002**, *4*, 311−316.

(3) Erickson, A. S.; Misra, S.; Miller, G. J.; Gupta, R. R.; Schlesinger, Z.; Harrison, W. A.; Kim, J. M.; Fisher, I. R. Ferromagnetism in the Mott Insulator Ba_2NaOsO_6. *Phys. Rev. Lett.* **2007**, *99* (1), 016404.

(4) Steele, A. J.; Baker, P. J.; Lancaster, T.; Pratt, F. L.; Franke, I.; Ghannadzadeh, S.; Goddard, P. A.; Hayes, W.; Prabhakaran, D.; Blundell, S. J. Low moment magnetism in the double perovskites Ba_2MOsO_6 (M = Li, Na). *Phys. Rev. B* **2011**, *84*, 144416.

(5) Lu, L.; Song, M.; Liu, W.; Reyes, A. P.; Kuhns, P.; Lee, H. O.; Fisher, I. R.; Mitrović, V. F. Magnetism and local symmetry breaking in a Mott insulator with strong spin orbit coupling. *Nat. Commun.* **2017**, *8*, 14407.

(6) Chen, G.; Pereira, R.; Balents, L. Exotic phases induced by strong spin-orbit coupling in ordered double perovskites. *Phys. Rev. B* **2010**, *82*, 174440.

(7) Svoboda, C.; Zhang, W.; Randeria, M.; Trivedi, N. Orbital order drives magnetic order in $5d^1$ and $5d^2$ double perovskite Mott insulators. *Phys. Rev. B* **2021**, *104*, 024437.

(8) Cong, R.; Nanguneri, R.; Rubenstein, B.; Mitrović, V. F. Evidence from first-principles calculations for orbital ordering in Ba_2NaOsO_6: A Mott insulator with strong spin-orbit coupling. *Phys. Rev. B* **2019**, *100* (24), 245141.

(9) Marjerrison, C. A.; Thompson, C. M.; Sala, G.; Maharaj, D. D.; Kermarrec, E.; Cai, Y.; Hallas, A. M.; Wilson, M. N.; Munsie, T. J. S.; Granroth, G. E.; Flacau, R.; Greedan, J. E.; Gaulin, B. D.; Luke, G. M. Cubic Re^{6+} ($5d^1$) Double Perovskites, Ba_2MgReO_6, Ba_2ZnReO_6, and $Ba_2Y_{2/3}ReO_6$: Magnetism, Heat Capacity, μSR, and Neutron Scattering Studies and Comparison with Theory. *Inorg. Chem.* **2016**, *55*, 10701−10713.

(10) Hirai, D.; Hiroi, Z. Successive Symmetry Breaking in a $J_{eff} = 3/2$ Quartet in the Spin−Orbit Coupled Insulator Ba_2MgReO_6. *J. Phys. Soc. Jpn.* **2019**, *88*, 064712.

(11) Hirai, D.; Sagayama, H.; Gao, S.; Ohsumi, H.; Chen, G.; Arima, T.; Hiroi, Z. Detection of multipolar orders in the spin-orbit-coupled *5d* Mott insulator Ba_2MgReO_6. *Phys. Rev. Res.* **2020**, *2* (2), 022063.

(12) Liu, W.; Cong, R.; Reyes, A. P.; Fisher, I. R.; Mitrović, V. F. Nature of lattice distortions in the cubic double perovskite Ba_2NaOsO_6. *Phys. Rev. B* **2018**, *97*, 224103.

(13) Cong, R.; Nanguneri, R.; Rubenstein, B.; Mitrović, V. F. First principles calculations of the electric field gradient tensors of Ba_2NaOsO_6, a Mott insulator with strong spin orbit coupling. *J. Phys.: Cond. Matter* **2020**, *32*, 405802.

(14) Coelho, A. A. TOPAS and TOPAS-Academic: an optimization program integrating computer algebra and crystallographic objects written in C++. *J. Appl. Crystallogr.* **2018**, *51*, 210−218.

(15) Momma, K.; Izumi, F. VESTA 3 for three−dimensional visualization of crystal, volumetric and morphology data. *J. Appl. Crystallogr.* **2011**, *44*, 1272−1276.

(16) Stokes, H. T.; Hatch, D. M.; Campbell, B. J. *ISODISTORT, ISOTROPY Software Suite* iso.byu.edu accessed 11 November 2024.

(17) Campbell, B. J.; Stokes, H. T.; Tanner, D. E.; Hatch, D. M. ISODISPLACE: An Internet Tool for Exploring Structural Distortions. *J. Appl. Crystallogr.* **2006**, *39*, 607−614.

(18) Bain, G. A.; Berry, J. F. Diamagnetic Corrections and Pascal's Constants. *J. Chem. Educ.* **2008**, *85*, 532.

(19) Vasala, S.; Karppinen, M. $A_2B'B''O_6$ perovskites: A review. *Prog. Solid State Chem.* **2015**, *43*, 1−36.

(20) Retuerto, M.; Martinez-Lope, M. J.; Garcia-Hernandez, M.; Fernandez-Diaz, M. T.; Alonso, J. A. Crystal and Magnetic Structure of Sr_2MReO_6 (M = Ni, Co, Zn) Double Perovskites: A Neutron Diffraction Study. *Eur. J. Inorg. Chem.* **2008**, *4*, 588−595.

(21) Glazer, A. M. Classification of tilted octahedra in perovskites *Acta Crystallogr. Sect. B* **1972**, *B28*, 3384.

(22) Dragomir, M.; Aczel, A. A.; Wiebe, C. R.; Lussier, J. A.; Dube, P.; Greedan, J. E. Magnetic ground state of La_2LiMoO_6: A comparison with other Mo^{5+} (S = 1/2) double perovskites. *Phys. Rev. Mater.* **2020**, *4*, 104406.

(23) Nilsen, G. J.; Thompson, C. M.; Marjerisson, C. A.; Badrtdinov, D. I.; Tsirlin, A. A.; Greedan, J. E. Magnetic order and multipoles in the $5d^2$ rhenium double perovskite Ba_2YReO_6. *Phys. Rev. B* **2021**, *103*, 104430.

(24) Xiong, J.; Yan, J.; Aczel, A. A.; Woodward, P. M. Exploring the role of structural distortions in double perovskites containing $5d^2$ ions. *J. Solid State Chem.* **2018**, *258*, 762−767.

(25) Kuwahara, K.; Iwasa, K.; Kohgi, M.; Aso, N.; Sera, M.; Iga, F. Detection of Neutron Scattering from Phase IV of $Ce_{0.7}La_{0.3}B_6$: A Confirmation of the Octupole Order. *J. Phys. Soc. Jpn.* **2007**, *76*, 093702.

(26) Shiina, R.; Sakai, O.; Shiba, H. Magnetic Form Factor of Elastic Neutron Scattering Expected for Octupolar Phases in $Ce_{1-x}La_xB_6$ and NpO_2. *J. Phys. Soc. Jpn.* **2007**, *76*, 094702.

(27) Tehrani, A. M.; Spaldin, N. A. Untangling the structural, magnetic dipole, and charge multipolar orders in Ba_2MgReO_6. *Phys. Rev. Mater.* **2021**, *5*, 104410.

(28) Arima, H.; Oshita, Y.; Hirai, D.; Hiroi, Z.; Matsubayashi, K. Interplay between Quadrupolar and Magnetic Interactions in $5d^1$ Double Perovskite Ba_2MgReO_6 under Pressure. *J. Phys. Soc. Jpn.* **2022**, *91*, 013702.

(29) Ma, C.-G.; Brik, M. G. Systematic analysis of spectroscopic characteristics of heavy metal transition metal ions with $4d^n$ and $5d^n$

(n = 1−10) electronic configurations in a free state. *J. Lumin.* **2014**, *145*, 402−409.
(30) Lovesey, S. W.; Khalyavin, D. D. Magnetic order and $5d^1$ multipoles in a rhenate double perovskite Ba_2MgReO_6. *Phys. Rev. B* **2021**, *103*, 235160.
(31) Ross, J. W.; Lam, D. J. The magnetic susceptibility of neptunium oxide and carbide between 4.2 and 300 K. *J. Appl. Phys.* **1967**, *38*, 1451−1453.
(32) Friedt, J. M.; Litterst, F. J.; Rebizant, J. 25 K Phase transition in NpO_2 from Np-237 Mossbauer spectroscopy. *Phys. Rev. B* **1985**, *32*, 257−263.
(33) Kopmann, W.; Litterst, F. J.; Klauss, H. H.; Hillberg, M.; Wagener, W.; Kalvius, G. M.; Schreier, E.; Burghart, F. J.; Rebizant, J.; Lander, G. H. Magnetic order in NpO_2 and UO_2 studied by muon spin rotation. *J. Alloys Comp.* **1998**, *271*, 463−466.
(34) Mannix, D.; Lander, G. H.; Rebizant, J.; Caciuffo, R.; Bernhoeft, N.; Lidstrom, E.; Vettier, C. Unusual magnetism of NpO_2: A study with resonant X-ray scattering. *Phys. Rev. B* **1999**, *60*, 15187−15183.
(35) Cox, D. E.; Frazer, B. C. A neutron diffraction study of NpO_2. *J. Phys. Chem. Solids* **1967**, *28*, 1649−1650.
(36) Frontzek, M. D.; Sadergaski, L. R.; Cary, S. K.; Rai, B. K. Search for octupolar order in NpO_2 by neutron powder diffraction. *J. Solid State Chem.* **2023**, *321*, 123875.
(37) Howard, C. J.; Kennedy, B. J.; Woodward, P. M. Structures of ordered double perovskites − A group theoretical analysis. *Acta Crystallogr., Sect. B* **2003**, *59*, 463−471.
(38) Lufaso, M. W.; Barnes, P. W.; Woodward, P. M. Crystal Structure Prediction of Ordered Double Perovskites: SPuDS II. *Acta Crystallogr., Sect. B* **2006**, *62*, 397−410.
(39) Ishikawa, H.; Hirai, D.; Ikeda, A.; Gen, M.; Yajima, T.; Matsuo, A.; Matsuda, Y. H.; Hiroi, Z.; Kindo, K. Phase transition in the $5d^1$ double perovskite Ba_2CaReO_6 induced by high magnetic field. *Phys. Rev. B* **2021**, *104*, 174422.
(40) Hirai, D.; Hiroi, Z. Possible quadrupole order in tetragonal Ba_2CdReO_6 and chemical trend in the ground states of $5d^1$ double perovskites. *J. Phys.: Condens. Matter* **2021**, *33*, 135603.
(41) Gao, S.; Hirai, D.; Sagayama, H.; Ohsumi, H.; Hiroi, Z.; Arima, T. H. Antiferromagnetic long-range order in the $5d^1$ double-perovskite Sr_2MgReO_6. *Phys. Rev. B* **2020**, *101* (22), 220412.
(42) Greedan, J. E.; Derakhshan, S.; Ramezanipour, F.; Siewenie, J.; Proffen, T. A search for disorder in the spin glass double perovskites Sr_2CaReO_6 and Sr_2MgReO_6 using neutron diffraction and neutron pair distribution function analysis. *J. Phys.: Condens. Matter* **2011**, *23*, 164213.

https://doi.org/10.1021/acs.chemmater.4c02135
Chem. Mater. 2024, 36, 11478−11489